Continuous Vortices with Broken Symmetry in Rotating Superfluid ^{3}He-A

H. K. Seppälä, P. J. Hakonen, M. Krusius, T. Ohmi,[a] M. M. Salomaa, and J. T. Simola
Low Temperature Laboratory, Helsinki University of Technology, SF-02150 Espoo 15, Finland

and

G. E. Volovik
L. D. Landau Institute for Theoretical Physics, U.S.S.R. Academy of Sciences, 117334 Moscow, U.S.S.R.
(Received 28 February 1984)

New NMR measurements are reported on continuous ^{3}He-A vortices in tilted magnetic fields. We introduce a symmetry classification of the continuous vortices with broken axial symmetry. It is found that the discrete internal symmetry may in addition be broken in two inequivalent ways, producing two different continuous vortices. Although NMR may not distinguish between these two vortices, the observed vortex satellite peak is well accounted for by spin waves localized in the soft core of such vortices.

PACS numbers: 67.50.Fi

Recent NMR experiments[1] have produced the first data on vortices in rotating superfluid ^{3}He. In particular, in the anisotropic A phase the NMR results suggest the presence of new vortices[2] which unlike vortices in He-II do not involve a superflow given simply by the gradient of phase. Instead, vorticity ($\nabla \times \vec{v}_s$) is continuously distributed and supported by smooth winding of the orbital part of the order parameter. In this Letter we report new NMR measurements, where the static magnetic field $H = 28.4$ mT is tilted by an angle μ with respect to the common orientation of the rotation axis $\hat{\Omega}$ and the axis $\hat{z}$ of the cylindrical sample. We also calculate the vortex texture numerically: Two distinct axially nonsymmetric continuous vortices are found, with different symmetries in the $\hat{l}$ texture but with their NMR signatures in good agreement with the observations.

Two topologically different types of vortices with continuous vorticity are relevant for ^{3}He-A as follows: (i) singular vortices with a hard-core radius of the order of the superfluid coherence length $\xi \sim 0.01$ μm inside which the A phase pairing amplitude tends to zero, and (ii) continuous vortices with no hard core and with A phase everywhere. In the present experiments, with magnetic fields larger than the dipolar field $H_D \sim 2.5$ mT, both kinds of vortices possess a soft core with a radius of the order of the dipole length $\xi_D \sim 10$ μm, within which the vorticity is concentrated.

In the measurements we study the effect of rotation on the transverse cw NMR absorption. The most prominent feature is an Ω-dependent line broadening. Close to T_c it is caused by spin diffusion and at lower temperatures primarily by the scattering of spin waves from vortices.[3] However, the crucial new feature of the NMR signal in the rotating state is a small satellite absorption peak, due to vortices. Its shift from the Larmor frequency f_0, $f_V - f_0$, is a weakly temperature-dependent fraction of the bulk A liquid shift $f_A - f_0$. The vortex shift $f_V - f_0$ is independent of Ω and H in the region of the measurements ($\Omega < 2$ rad/s and $H = 10$–30 mT), and it does not depend on the orientation of $\vec{H}$ either, as is illustrated by the data in Fig. 1.

Spin-wave resonance absorption due to localized modes in the dipole-unlocked soft cores causes the vortex satellite. The structure of the soft core is not affected by the vortex density; consequently, $f_V - f_0$ is insensitive to Ω . The integrated NMR absorption of the satellite peak I_V, on the other hand, reflects the number of vortices and is propor-

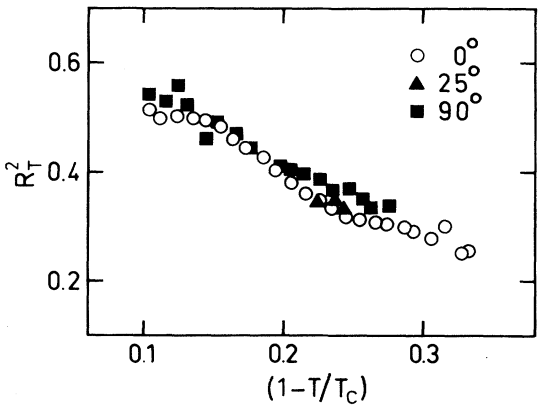

FIG. 1. Frequency shift $f_V - f_0$ of the vortex satellite in terms of $R_f^2 \sim 2f_0(f_V - f_0)/(f_L^A)^2$ at 29.3 bars as a function of temperature with $H = 28.4$ mT orientated at three different angles μ with respect to $\hat{\Omega}$.

tional to Ω, as seen in Fig. 2. Contrary to $f_V - f_0$, I_V appears nearly temperature independent which may be understood as a cancellation of the drop in $R_T^2 = (f_V^2 - f_0^2)/(f_L^4)^2$ (c.f. Fig. 1) and the increase in ξ_D resulting in an increase in the soft-core radius with decreasing temperature. Observe that I_V provides a more sensitive probe of the core structure than the shift $f_V - f_0$ as is illustrated in the dependence on $\vec{H}$ in Figs. 1 and 2.

Unlike in the ^{3}He-B experiments,[1] no time lag is observed between the satellite absorption intensity and the rotation speed during acceleration or deceleration within the time scale of the cw NMR measurement (signal averaging limits the time resolution to 1 s). This is a strong indication in favor of continuous vortices. Furthermore, the calculated values of $f_V - f_0$ and $I_V/(I_{\rm tot}\Omega)$ are closer to the experimental results in continuous vortex models; typically $R_T^2 \sim 0.5$ and $I_V/(I_{\rm tot}\Omega) \sim 0.05$ while for singular vortices larger values, $R_T^2 \sim 1$ and $I_V/(I_{\rm tot}\Omega) \sim 0.5$, are obtained. This is due to the shallower spin-wave potential of singular vortices and the correspondingly more extended spin waves spreading well beyond the soft core.

Outside the core, superflow restricts $\hat{l}$ to the plane perpendicular to $\hat{\Omega}$, while $\hat{d}$ is confined to the plane perpendicular to $\vec{H}$. Tilting $\vec{H}$ away from the rotation axis fixes the orientation for the common dipole-locked axis of $\hat{l}$ and $\hat{d}$ as the intersection of the two planes. The slight deviation from a uniform $\hat{l}$ field and the spontaneous distortion of the vortex lattice along $\hat{l}$ are discussed by Ohmi.[4] Quantitative agreement with the NMR measurement is obtained by simply assuming that the uniform $\hat{d}$ field extends over the core, and thus the net effect of tilting $\vec{H}$ is only to fix the $\hat{l}$ and $\hat{d}$ orientations without causing changes in the $\hat{l}$ field. Indeed, this interpretation is supported by the frequency-shift data in Fig. 1. However, the absorption data in Fig. 2 do not conform to this picture. In addition to a slight μ dependence of the texture, this is partly associated with the fact that the total rf absorption $I_{\rm tot}$ decreases below its stationary-state value linearly with Ω when μ deviates from zero. Since the missing rf absorption is proportional to $I_V(\Omega)$, we infer that it is transferred to the longitudinal NMR mode.

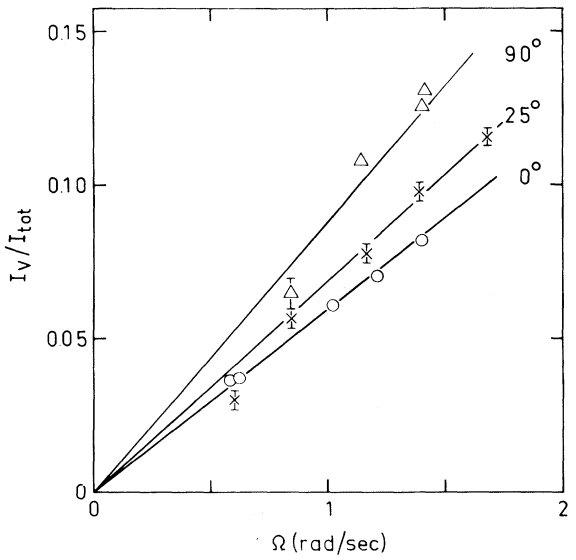

FIG. 2. Integrated NMR absorption I_V of the vortex satellite as a function of Ω for $1 - T/T_c = 0.22$–0.25. The I_V is normalized to the measured total absorption $I_{\rm tot}$ simultaneously.

Let us now classify the symmetries of the continuous vortices using the approach of Salomaa and Volovik.[5] Consider the simple singular-phase vortex with two quanta of circulation located in a uniform $\hat{l}$ field along $\hat{x}$. Writing the order parameter as $A_{\alpha i} \propto d_\alpha(\Delta_i' + i\Delta_i'')$ with $\hat{l} = \hat{\Delta}' \times \hat{\Delta}''$, we represent the vortex as

$$A_{\alpha i} = C(r)\hat{x}_\alpha(\hat{y}_i + i\hat{z}_i)e^{-2i\phi}, \tag{1}$$

where x,y,z and r,ϕ,z are Cartesian and cylindrical coordinates. The amplitude $C(r)$ vanishes in the hard core, $C(r \to 0) \to 0$. This vortex is invariant under the discrete symmetry operations of the symmetry group $Z_2 \times Z_2$ with four elements as follows:

$$1, \quad P_1 = e^{i\pi}P, \quad P_3 = e^{i\pi}TO^J_{y,\pi}, \qquad P_2 = P_1P_3 = TPO^J_{y,\pi}. \tag{2}$$

Here P denotes parity transformation $PA_{\alpha i}(\vec{r}) = -A_{\alpha i}(-\vec{r})$, T represents time inversion $TA_{\alpha i} = A^*_{\alpha i}$, $O^J_{y,\pi}$ describes combined rotation of the spin and orbital spaces about y through π, and $e^{i\pi}$ is a gauge transformation. The same elements of symmetry remain in a tilted field if one assumes that the tilting of H does not change the texture.

The vortex in Eq. (1), which represents the asymptotic form of the continuous vortices at large r, is unstable with respect to perturbations breaking space parity P, which transforms this singular vortex into a continuous one with lower energy.[6] The symmetry P may be broken in two different ways: either P_2 or P_3 may be conserved. Following Ref. 5, we call these vortices v and w. We use the trial functions[2]

$$\vec{\Delta}' + i\vec{\Delta}'' = [(\hat{z}\sin\Phi + \hat{y}\cos\Phi)\sin\eta + \hat{x}\cos\eta + i(-\hat{y}\sin\Phi + \hat{z}\cos\Phi)]e^{-i\Phi}, \tag{3}$$

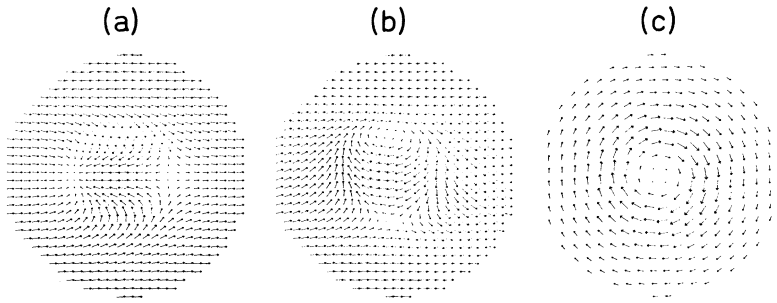

FIG. 3. The $\hat{l}$ and $\vec{v}_s$ fields of the continuous vortices with two quanta of circulation: (a) v vortex with symmetry P_2, and (b) w vortex with symmetry P_3. The arrows show $\hat{l}$ projected into the x-y plane perpendicular to $\hat{\Omega}$; $\vec{H}$ is along $\hat{\Omega}$ while $\hat{d}$ is along $\hat{x}$. (c) $\vec{v}_s$ is practically indistinguishable for both vortex textures; arrows depict $\vec{v}_s = (\hbar/2m_3)[\hat{\Delta}' \cdot (\partial\hat{\Delta}''/\partial x)\hat{x} + \hat{\Delta}' \cdot (\partial\hat{\Delta}''/\partial y)\hat{y}]$. The radii of the circles are $5\xi_D$.

where the phase $\Phi = \phi + \phi_0$ is chosen such that $\phi_0 = -\pi/2$ for the P_2 symmetric v vortex and $\phi_0 = 0$ for the P_3 symmetric w vortex, and $\eta(\vec{r})$ is a trial function with $\eta(\vec{r} = \infty) = -\eta(\vec{r} = 0) = \pi/2$. Note that any observable physical property exhibits the nonconservation of parity P. We minimize the dipole and gradient energies with respect to $\eta(\vec{r})$.[7] The vortex energy per unit length is written as[2] $F_V = \pi\rho_s(\hbar/2m_3)^2[3\ln(R/\xi_D) + C - \frac{9}{4}]$, where R is the radius of the Wigner-Seitz cell of the vortex lattice and C contains the gradient and dipole contributions primarily from the soft core. Solving the two-dimensional Euler-Lagrange equations for $\eta(\vec{r})$ gives $C^v = 1.6$ and $C^w = 1.1$. The resulting $\hat{l}$ textures are shown in Figs. 3(a) and 3(b), respectively.

The topological constraint on the continuous vortex requires that $\hat{l}$ traverses through all points on the unit sphere. In both the v and w vortices there exist two points where $\hat{l}$ is along the rotation axis, $\hat{l} = \pm\hat{z}$. These points may be regarded as the centers of 2π Mermin-Ho vortices. In zero field the Mermin-Ho vortices form a lattice,[4] whereas at high fields they cluster into bound pairs forming 4π Anderson-Toulouse-Chechetkin types of vortices.[1] These vortex pairs have an analogy in the "instanton quarks"—a pair forming an instanton.[8] In the v vortex, called "radial hyperbolic" by Maki,[9] the pair axis lies along $\hat{x} \parallel \hat{d}$. In the w vortex ("circular hyperbolic"), the pair axis is perpendicular to $\hat{d}$. However, such projections do not provide unique characterization: Plotting $l_x(x,y)$ and $l_z(x,y)$ [instead of $l_x(x,y)$ and $l_y(x,y)$] for the w vortex we reproduce the pattern shown in Fig. 3(a), while a similar projection of the v vortex gives Fig. 3(b) rotated by 180°. Both vortices have practically identical projections of the $\vec{v}_s$ field, shown in Fig. 3(c). Thus v and w vortices have related stereometric structures, but differ in their orientations. A representation of this 4π vortex structure in terms of a "radial-hyperbolic" or "circular-hyperbolic" pair is therefore arbitrary.

The transverse (T) spin-wave frequency is found by solving the resonance fluctuations of $\hat{d}$, yielding $R_T^2 - 1$ as the eigenvalue of the lowest state. In a uniform $\hat{d}$ texture the transverse spin-wave potential is $V_T = -(l_y^2 + 2l_z^2)$. This potential is the double well shown in Fig. 4. The two minima lie at $\hat{l} = \pm\hat{z}$. The w vortex potential is identical, only rotated by 90° to make the minima coincide with the locations $\hat{l} = \pm\hat{z}$ in Fig. 3(b). [In longitudinal (L) NMR, the spin-wave potential is $V_L = -(2l_y^2 + l_z^2)$, and now the points with $\hat{l} = \pm\hat{y}$ correspond to the minima; hence $V_L^v \simeq V_T^w$.] The calculated eigenvalues are $R_T^2 = 0.48$ and 0.57 for the v and w vor-

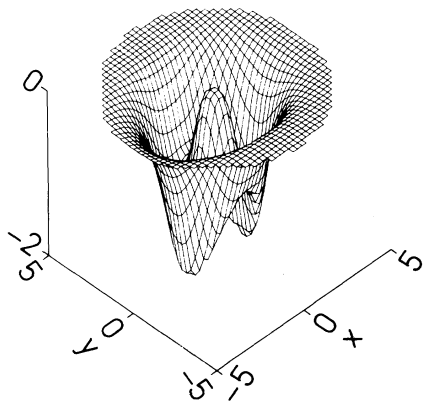

FIG. 4. The potential well $V_T^v = -(2l_z^2 + l_y^2)$ for transverse spin-wave modes of the v vortex. Approximately, the potential V_T^w for the w vortex is obtained by a 90° rotation about $\hat{\Omega}$.

tices, while the respective normalized weights of the wave functions yield $I_V/(I_{\rm tot}\Omega)=0.035$ and 0.038. The experimental values, extrapolated to T_c, are $R_T^2=0.70\pm0.10$ and $I_V/(I_{\rm tot}\Omega)=0.060\pm0.010$, if one assumes R_T to vary linearly with temperature[1] and the intensity to be constant.

In conclusion, it appears that magnetic measurements will not resolve between the two closely surements will not resolve between the two closely similar vortex textures of Fig. 3. It has been pointed out by Volovik[10] that the broken-symmetry properties of the v vortex give rise to a spontaneous electric polarization directed along the vortex axis, while the w vortex instead displays a spontaneous supercurrent along the vortex axis. For experimental purposes the predicted value of the electric dipole moment is small. Moreover, since it is proportional to the soft-core area, the dipole moment is maximal in zero field, where, however, the vortex pairs separate into a lattice of Mermin-Ho vortices.

We thank I. A. Fomin and K. Maki for discussions. This work was supported by the Academy of Finland.

[a]Permanent address: Department of Physics, Kyoto University, Kyoto 606, Japan.

[1]P. J. Hakonen, O. T. Ikkala, S. T. Islander, O. V. Lounasmaa, and G. E. Volovik, J. Low Temp. Phys. **53**, 425 (1983).

[2]H. K. Seppälä and G. E. Volovik, J. Low Temp. Phys. **51**, 279 (1983).

[3]I. A. Fromin and V. G. Kamenskij, Pis'ma Zh. Eksp. Teor. Fiz. **35**, 241 (1982) [JETP Lett. **35**, 302 (1982)].

[4]T. Ohmi, to be published.

[5]M. M. Salomaa and G. E. Volovik, Phys. Rev. Lett. **51**, 2040 (1983), and to be published.

[6]Singular-vortex solutions exist which are lower in energy at low Ω than continuous vortices (see Ref. 2).

[7]It is found that deviations of $\hat{d}$ from uniformity are small and of little consequence to the $\hat{l}$ texture. The energy values quoted are for the case where $\hat{d}$ is allowed to change. The lower dipole energy and the two-dimensional minimization reduce the present C values below $C^v=2.0$ given in Ref. 2.

[8]V. A. Fateyev, I. V. Frolov, and A. S. Schwarz, Nucl. Phys. B **154**, 1 (1979).

[9]X. Zotos and K. Maki, to be published.

[10]G. E. Volovik, Pis'ma Zh. Eksp. Teor. Fiz. **39**, 169 (1984).